ELSEVIER

Journal of Power Sources 97–98 (2001) 298–302

JOURNAL OF POWER SOURCES

www.elsevier.com/locate/jpowsour

Physical and electrochemical characterization of $LiNi_{0.8}Co_{0.2}O_2$ thin-film electrodes deposited by laser ablation

G.X. Wang*, M.J. Lindsay, M. Ionescu, D.H. Bradhurst, S.X. Dou, H.K. Liu

Energy Storage Materials Research Program, Institute for Superconducting & Electronic Materials, University of Wollongong, NSW 2522, Australia

Received 11 July 2000; accepted 4 January 2001

Abstract

The thin-film electrodes of $LiNi_{0.8}Co_{0.2}O_2$ were deposited by pulsed laser ablation. The average thickness of these thin-films was measured by AFM to be approximately 0.62 μm. The electrochemical properties of $LiNi_{0.8}Co_{0.2}O_2$ thin-films as working electrode in lithium cells were characterized by galvanostatic charge/discharge, cyclic voltammetry and ac impedance spectroscopy. The average capacity of these thin-film electrodes is about 60–62.5 $\mu A/cm^2$ μm. The Li^+ diffusion coefficient in the $LiNi_{0.8}Co_{0.2}O_2$ thin-film electrode was measured to be in the range of 3.19×10^{-13}–2.48×10^{-10} m^2/s.

Keywords: $LiNi_{0.8}Co_{0.2}O_2$; Thin-film; Laser ablation; Lithium-ion battery

1. Introduction

Lithium ion batteries are state-of-the-art power sources for portable telecommunication and electronic devices. Thin-film lithium ion microbatteries have been developed for several years. These microbatteries can be used as an integral part of micro-electronic circuits (on-chip CMOS memory backup) or the miniature electronics such as micro-mechanics, miniature hearing aids and implanted medical devices [1–4]. Thin-films of oxides can be made by many techniques. Of these, laser ablation is a new and powerful technology to produce films. It can directly deposit film on the metal substrate without the requirement of a buffer layer and post-heat treatment.

In this investigation, we prepared $LiNi_{0.8}Co_{0.2}O_2$ thin-film electrodes using pulsed laser ablation technique. The $LiNi_{0.8}Co_{0.2}O_2$ compound has the potential to be used as a cathode material instead of $LiCoO_2$, because it is cheaper, less toxic and has higher capacity than $LiCoO_2$ [5,6]. Thin-film electrodes provide an ideal geometry for fundamental research on electrode materials, and overcome the uncertainties of porous powder electrodes. The electrochemical properties of $LiNi_{0.8}Co_{0.2}O_2$ thin-film electrodes were characterized using lithium test cells.

2. Experimental

$LiNi_{0.8}Co_{0.2}O_2$ thin-films were deposited on a nickel substrate by pulsed laser ablation. $LiNi_{0.8}Co_{0.2}O_2$ powders (Merck, Germany) were pressed into pellets and sintered at 900°C for 24 h as the target. The laser ablation system is an Excimer Laser LAMBDA PHYSIK, Complex 301 with $\lambda = 248$ nm, 1–10 Hz, 1.2 J/pulse maximum energy output. The incidence angle between direction and target is 45°C. During deposition, the target was rotated at 10 rpm and the substrate was mounted on a holder which was resistively heated to 600°C. Films were deposited for 30 min under an oxygen pressure of 100 mTorr, using a 5 Hz, 450 mJ/pulse KF laser. The thickness and morphology of the thin-films were measured and observed by AFM microscopy. The phase structure of $LiNi_{0.8}Co_{0.2}O_2$ thin-films was analyzed by X-ray diffraction. The lithium test cells were assembled in an argon filled glove-box using the $LiNi_{0.8}Co_{0.2}O_2$ thin-film as cathode, lithium foil as counter electrode and reference electrode. The electrochemical properties of thin-film electrodes were examined via galvanostatic charge/discharge, cyclic voltammetry and ac impedance spectroscopy.

3. Results and discussions

3.1. Physical characterization of $LiNi_{0.8}Co_{0.2}O_2$ thin-films

Fig. 1(a) shows the X-ray diffraction patterns of a $LiNi_{0.8}Co_{0.2}O_2$ thin-film and target. The diffraction lines

* Corresponding author. Fax: +61-2-42216731.
E-mail address: gw14@uow.edu.au (G.X. Wang).

0378-7753/01/$ – see front matter
PII: S0378-7753(01)00664-4

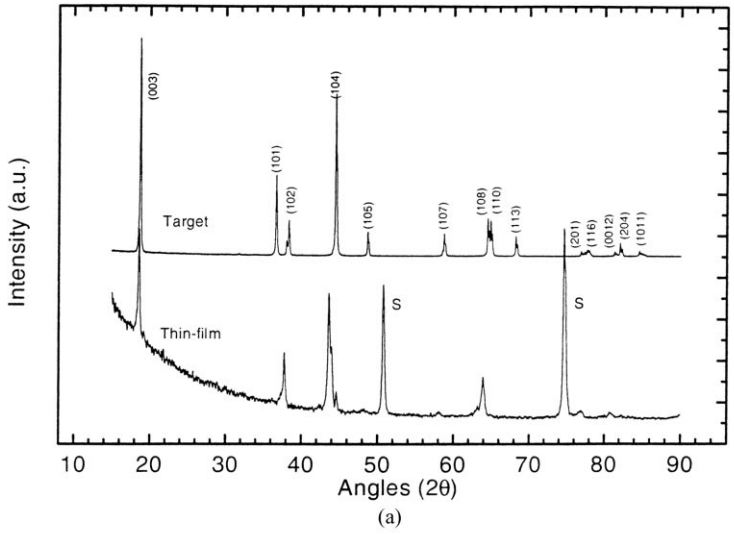

(a)

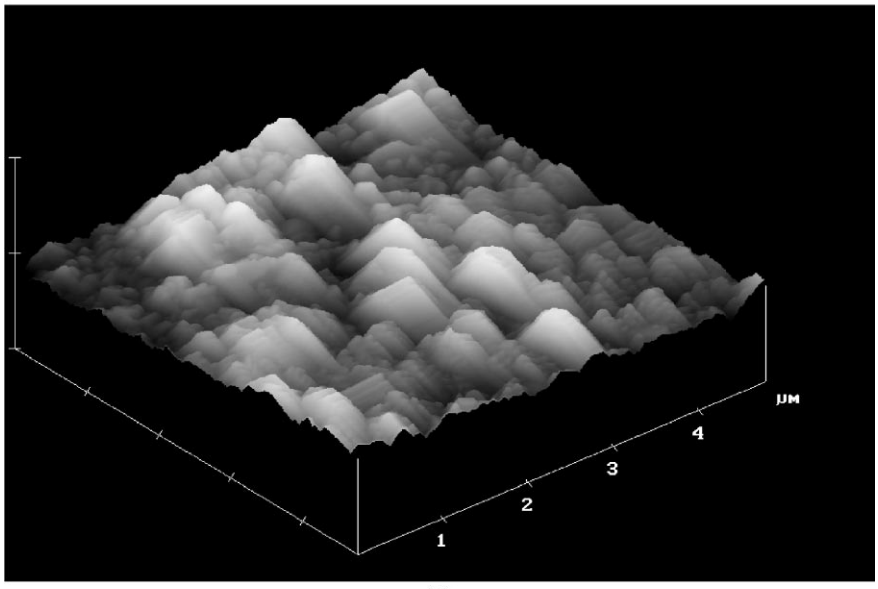

(b)

Fig. 1. (a) X-ray diffraction patterns of a $LiNi_{0.8}Co_{0.2}O_2$ thin-film and target. (b) AFM image of $LiNi_{0.8}Co_{0.2}O_2$ thin-film.

from the substrate were marked with S. Compared to the XRD pattern of the target, some diffraction peaks of the thin-film disappeared or became indistinguishable. This probably is ascribed to the formation of texture in the thin-film. Nevertheless, the hexagonal structure can be identified for $LiNi_{0.8}Co_{0.2}O_2$ thin-films.

The morphology of as deposited thin-films was observed by AFM microscopy. As shown in Fig. 1(b), the roughness of the thin-films varies in micro-domain. The thickness of the thin-films was measured by AFM to be about 620 nm. In macro-domain, the thin-films seem to be deposited homogeneously.

3.2. Electrochemical properties of $LiNi_{0.8}Co_{0.2}O_2$ thin-films

The capacity of $LiNi_{0.8}Co_{0.2}O_2$ thin-film electrode was examined by constant current charge/discharge. Four test cells were assembled and cycled in the voltage range of 3.0–4.3 V at a constant current density of 10 μA/cm^2. Fig. 2(a) shows the voltage versus capacity profile of the first charge/discharge. A capacity of 60.3–62.5 μAh/cm^2 μm can be delivered in the first discharge. This corresponds to a specific capacity of approximately 125 mAh/g (assuming that the $LiNi_{0.8}Co_{0.2}O_2$ thin-film had no porosity and a theoretical density of 4.8 g/cm^3). In the first cycle, the efficiency (ratio of discharge capacity to charge capacity) is about 86.2%. Some charging current may be consumed by the side reaction. Because Ni in the Ni^{4+} state is very reactive, this could cause the decomposition of the organic electrolyte. A passivation product could be formed on the surface of the thin-film electrode, but the nature of this process is unclear so far. From the second cycle, the capacity of the thin-film electrode gradually declined. However, the efficiency of cycling was improved and maintained

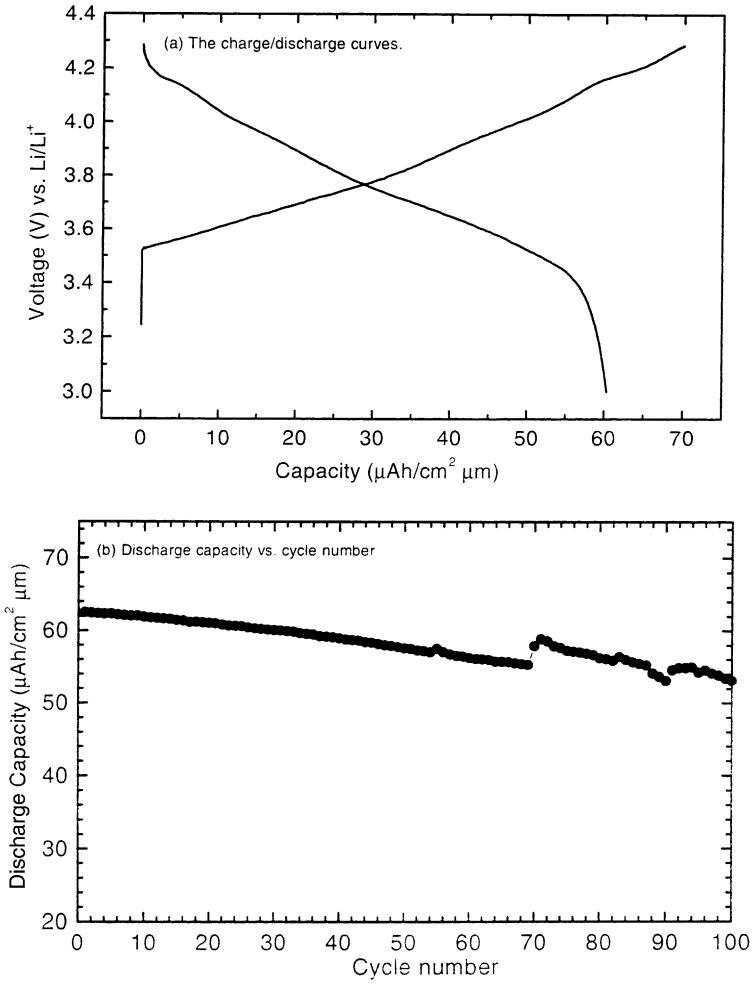

Fig. 2. (a) Charge/discharge curves of $LiNi_{0.8}Co_{0.2}O_2$ thin-film electrode. (b) Discharge capacity of $LiNi_{0.8}Co_{0.2}O_2$ thin-film electrode vs. cycle number.

at 94% for each cycle. After 100 cycles, the capacity of the thin-film electrode still retained 85% of its first cycle value. This shows that the $LiNi_{0.8}Co_{0.2}O_2$ thin-film deposited by laser ablation technique demonstrated a reasonable capacity and good capacity retention. Further optimization of the thickness of thin-films and deposition conditions will probably improve the cyclability of thin-film electrodes.

Cyclic voltammetry measurements were performed on a $LiNi_{0.8}Co_{0.2}O_2$ thin-film electrode at a sweeping rate of 0.1 mV/s over a voltage range of 2.8–4.4 V. The cyclic voltammogram is shown in Fig. 3(a). Four anodic peaks were observed during the charging process (Li-ion extraction from the $LiNi_{0.8}Co_{0.2}O_2$ thin-film electrode). These four peaks are at 3.71, 3.91, 4.0 and 4.19 V, respectively. Correspondingly, in the process of discharging (Li-ion insertion into the $LiNi_{0.8}Co_{0.2}O_2$ thin-film electrode), four cathodic peaks were also observed which are at 3.66, 3.90, 3.98 and 4.16 V. On the average. cathodic peaks are 10–50 mV lower than the anodic peaks. These four paired peaks are attributed to the insertion/extraction reactions of Li ions in $LiNi_{0.8}Co_{0.2}O_2$ occurs in four different phase regions. Ohzuku et al. [7] found that there were four regions for the reaction of $LiNiO_2$ and $LiNi_{0.5}Co_{0.5}O_2$ electrodes in lithium cells with an electrolyte of 1 M $LiClO_4$ in propylene carbonate (PC). In region (I) for $0 < x < 0.25$, the reaction takes place in the rhombohedral phase; in region (II) for $0.25 \leq x \leq 1.0$, the reaction occurs in a monoclinic phase; in region (III) for $0.55 < x \leq 0.75$, the reaction proceeds in a rhombohedral phase; in region (IV) for $0.75 < x < 1.0$, the reaction consists of a rhombohedral two-phase reaction [7,8]. The results of our observation for $LiNi_{0.8}Co_{0.2}O_2$ thin-film using cyclic voltammetry measurement are similar to Ohzuku's investigation via XRD and differential chronopotentiograms. Since no binder or conduction additives were used in the thin-film electrodes, the identification of the electrochemical characterization using thin-film electrodes would be more accurate than that using porous, powder pressed electrodes. Cyclic voltamograms obtained from thin-film electrodes clearly demonstrated four oxidation and reduction peaks, which are a unique characteristic of $LiNi_{1-x}Co_xO_2$ compounds.

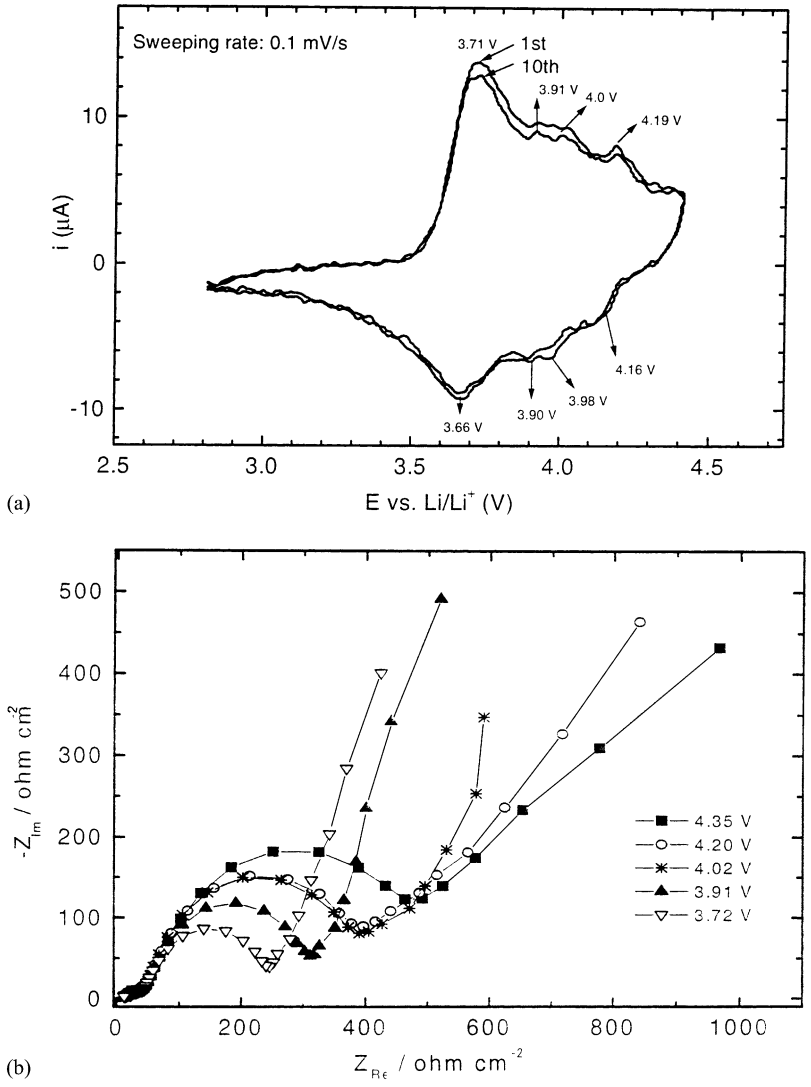

Fig. 3. (a) Cyclic voltamograms of $LiNi_{0.8}Co_{0.2}O_2$ thin-film electrode. (b) The ac impedance spectra of $LiNi_{0.8}Co_{0.2}O_2$ thin-film electrode.

To investigate the kinetics of lithium intercalation in $LiNi_{0.8}Co_{0.2}O_2$ thin-films and the characteristics of the thin-film/electrolyte interface ac impedance measurements were carried out on a $LiNi_{0.8}Co_{0.2}O_2$ thin-film electrode in different states. The thin-film electrode was potentiostatically conditioned at different potentials versus Li/Li^+ reference electrode. After a certain time of equilibrium, ac perturbation (5 mV) was applied to the thin-film electrode. The frequency was in the range of 100 kHz–1 mHz. Typical ac impedance spectra are shown in Fig. 3(b).

In general two semicircles were observed in the ac impedance spectra, which explicitly reflect well separated, different time constants of Li ion insertion processes in the $LiNi_{0.8}Co_{0.2}O_2$ thin-film. The high frequency semicircle is independent from the potential of the electrode. This semicircle is attributed to the formation of a surface layer on the electrode, caused either by the electrolyte decomposition product or the adsorption species. When Li^+ ions are electrochemically extracted from $LiNi_{0.8}Co_{0.2}O_2$, Ni^{3+} or Co^{3+} ions are oxidized to Ni^{4+} or Co^{4+}. Ni^{4+} or Co^{4+} ions are very reactive in nature and tend to react with the organic electrolyte, causing the decomposition product deposited on the surface of the electrode to form a passivation film. The medium frequency semicircle is assigned to charge-transfer resistance and non-Faradaic process occurring at the thin-film electrolyte interface related to slow Li^+ interfacial transfer. The low frequency range is diffusion-controlled process by Warburg impedance (Z_w). In the case of semi-infinite diffusion ($\omega \geq l^2$), the Warburg impedance can be expressed as

$$Z_w = \sigma\omega^{-1/2} - j\sigma\omega^{-1/2}$$

where σ is the Warburg pre-factor and ω is the angular frequency. The chemical diffusion coefficient D_{Li^+} at

different potentials may be deduced from the following relationship:

$$D_{Li^+} = \frac{1}{2}\left[\frac{V_m}{S}F\sigma \times \frac{dE}{dx}\right]^2$$

where dE/dx is the slope of the curve of voltage versus x in $Li_{1-x}Ni_{0.8}Co_{0.2}O_2$ which can be deduced from the charge/discharge curves in Fig. 2. V_m is the molar volume of the $LiNi_{0.8}Co_{0.2}O_2$ compound ($\sim$20.4 cm^3) and S is the area of the electrode. F is the Faraday constant. The variation of D_{Li^+} is in the range of 3.19×10^{-13}–2.48×10^{-10} m^2/s, in agreement with the diffusion coefficient reported in the literature for lithium insertion materials [9,10].

4. Conclusions

$LiNi_{0.8}Co_{0.2}O_2$ thin-films have been successfully prepared using a pulsed laser deposition technique which can allow direct deposition without any buffer layer or post heat treatment. The $LiNi_{0.8}Co_{0.2}O_2$ thin-film with a thickness of 0.62 μm can deliver a capacity of 60–62.5 μAh/cm^2. The thin-film electrode provides an ideal geometry for electrochemical characterization of electrode materials because it can eliminate any structurally-related side effects caused by a porous powder electrode. In the cyclic voltammetry measurement, four oxidation and reduction peaks were distinguished, which represent four different phase regions during insertion and extraction of Li^+ ion in $LiNi_{0.8}Co_{0.2}O_2$. Through ac impedance characterization, the lithium diffusion coefficient D_{Li^+} was measured to be in the range of 3.19×10^{-13}–2.48×10^{-10} m^2/s at different potentials.

References

[1] J.B. Bates, N.J. Dudney, D.C. Lubben, G.R. Gruzalski, B.S. Kwak, Xiaohua Yu, R.A. Zuhr, J. Power Sources 54 (1995) 58–62.
[2] K.A. Striebel, C.Z. Deng, S.J. Wen, E.J. Cairns, J. Electrochem. Soc. 143 (1996) 1821–1827.
[3] Steven D. Jones, James R. Akridge, Solid State Ionics 69 (1994) 357–368.
[4] T. Brousse, R. Retoux, U. Herterich, D.M. Schleich, J. Electrochem. Soc. 145 (1998) 1–4.
[5] R.V. Moshtev, P. Zlatilova, V. Manev, Atsushi Sato, J. Power Sources 54 (1995) 329–333.
[6] Shuji Yamada, Masashi Fujiwara, Motoya Kanda, J. Power Sources 54 (1995) 209–213.
[7] Tsutomu Ohzuku, Atsushi Ueda, Masatoshi Naavama, J. Electrochem. Soc. 140 (1993) 1862–1870.
[8] Atsushi Ueda, Tsutomu Ohzuku, J. Electrochem. Soc. 141 (1994) 2010–2014.
[9] P. Arora, B.N. Popov, R.E. White, J. Electrochem. Soc. 145 (1998) 1151.
[10] C. Bohnke, O. Bohnke, J.L. Fourquet, J. Electrochem. Soc. 144 (1997) 1151.